Fall 2014

Modeling of multi-terminal VSC-based HVDC systems

Mohammed Mabrook Alharbi

Department:

MODELING OF MULTI-TERMINAL VSC-BASED HVDC SYSTEMS

by

MOHAMMED MABROOK ALHARBI

A THESIS

Presented to the Graduate Faculty of the

MISSOURI UNIVERSITY OF SCIENCE AND TECHNOLOGY

In Partial Fulfillment of the Requirements for the Degree

MASTER OF SCIENCE IN ELECTRICAL ENGINEERING

2014

Approved by

Dr. M. Crow, Advisor
Dr. J. Kimball
Dr. M. Ferdowsi

ABSTRACT

Improving the efficiency and operation of power transmission is important due to the continual increase in demand for electric power. In addition, many remote areas throughout the world lack sufficient access to electricity. Unfortunately, utilities cannot satisfy the high demand of power by building new power stations because of economic and environmental reasons. However, utilities can increase generation and transmission line efficiencies by controlling the power flow through their systems. One new attractive technology that enables the control of power flow in the system is Voltage-Source-Converter High Voltage Direct Current (VSC-HVDC) transmission.

Multi-terminal-HVDC (M-HVDC) can be built using VSC technology. A model of a three-terminal VSC-HVDC system is presented in this thesis. One of the converters is used to regulate the DC voltage while the others converters control the active power independently and bi-directionally. The vector control strategy and pulse width modulation (PWM) technique are described and implemented in PSCAD/EMTDC. In addition, the region of controllability as a function of power flow has been analyzed. Furthermore, the steady-state and dynamic response characteristics as a function of capacitor size has been investigated.

ACKNOWLEDGMENTS

First and foremost, I express my sincere gratitude to my research advisor, Dr. Mariesa Crow, for the valuable guidance and help me for both my graduate study and writing this thesis. In addition, I would like to thank her for providing all needed facilities and related books. This work would not have been done without her efforts. I would like also to thank my committee members, Dr. Jonathan Kimball and Dr. Mehdi Ferdowsi, for attending as members on my thesis committee. Special thanks also to Darshit Shah for his help in this work. I would like also to thank my closest friend, Moneer Almalki, for being my stress release and supportive.

Financial assistance from Saudi Arabian Cultural Mission (SACM) in the form of research assistantship is grateful acknowledged. Besides, I extend my sincere thanks to King Saud University who afforded me a full scholarship for master's degree. I appreciate their supporting and confidence in me.

I also extend a very special acknowledgement to my parents for their encouragement and motivation. I always owe them keeping my work at the highest level until reach their dream of me. I dedicate this thesis to my wife, Sabah Altargmy, for being supportive and loving. I also dedicate this thesis to my little boy, Nawaf, for being patient and understanding.

TABLE OF CONTENTS

Page

LIST OF ILLUSTRATIONS

LIST OF TABLES

1. INTRODUCTION

Improving the efficiency and operation of energy transmission is important due to the continual increase in demand for electric power. In addition, many remote areas throughout the world lack sufficient access to electricity. Unfortunately, utilities cannot satisfy the high demand of power by building new power stations because of economic and environmental reasons. However, utilities can increase generation and transmission line efficiencies by controlling the power flow through their systems. One attractive technology that enables the control of power flow in the system is High Voltage Direct Current (HVDC) transmission.

HVDC links provide a good solution for transmitting power over long distances. Typically, HVDC links are primarily used for very long interconnections, asynchronous interconnections (to connect different frequencies or maintain synchronism), and power flow control. The conventional HVDC scheme, which utilizes thyristors, is commonly used to interconnect two AC systems. However, traditional thyristor-based HVDC systems have several limitations and undesirable characteristics such as being physically large and requiring a strong AC network [1]. Recently, voltage-source-converter-based high voltage direct current (VSC-HVDC) technology has been developed to overcome the disadvantages associated with the conventional HVDC systems. VSC-HVDC technology employs modern semiconductor technologies, such as the IGBT, that have the ability to turn-on and turn-off with much higher frequencies. This enables the VSC-HVDC to use vector control to obtain independent control of the active and reactive power flow using a DQ transformation. Pulse-width modulation (PWM) techniques are

then used to create the desired voltage waveform thus making it possible to obtain high performance of the converters and reduce harmonics. Therefore, VSC-HVDC technology has considerable potential to increase power system transmission capability over long distances and control active and reactive power flow independently.

In contrast to the conventional two-terminal point-to-point HVDC connection, it is straightforward to make multi-terminal connections in VSC-HVDC systems. Multi-terminal HVDC (M-HVDC) links connect more than two converters together providing additional reliability through the ability to compensate for the loss of any single converter in the system.

Many papers have been published on different aspects of VSC-HVDC systems. In [1], the analysis of harmonics in subsea power transmission cables used in VSC-HVDC has been investigated and a mathematical model of VSC-HVDC system has been developed. Analytic studies of interarea oscillation damping using active power modulation of three- and four-terminal HVDC transmission have been presented in [2]. The operation and control of a M-VSC-HVDC system for offshore wind farms has been investigated using a designed droop-based control scheme in [3]. New models have been presented for the STATCOM and VSC-HVDC aimed at power systems state estimation applications in [4]. A three phase dynamic phasor model of HVDC systems has been proposed to solve the dynamic characteristics of the converters for symmetrical and asymmetrical faults conditions in [5]. In [6], a model of VSC-HVDC system has been proposed for optimal power flow solutions using a Newton-Raphson algorithm. DC overvoltage control has been investigated during the loss of converter in a M-VSC-HVDC in [7].

This thesis focuses on the development of an independent control of the active power flow and DC link voltage of a M-HVDC system. The region of controllability as a function of power flow will be analyzed. Furthermore, the steady-state and dynamic response characteristics as a function of capacitor size will be investigated.

2. CONVENTIONAL HVDC AND VSC-HVDC SYSTEMS

2.1. INTRODUCTION

HVDC technology is a high power electronics technology developed to increase the efficiency of power transmission for long distances. In the 1950s, the Current-Source Converter (CSC) (shown in Figure 2.1) was introduced as the first conventional HVDC technology [8]. This type of HVDC utilizes thyristor valves to control power flow by maintaining the DC current flow in one direction and controlling the direction of active power flow with the polarity of the DC voltage [9]. In 2000, the first uses of Insulated-Gate Bipolar Transistor (IGBT) valves for HVDC was deployed in Australia with a 59 km, 180 MW, 80kV line [8]. This type of voltage source converter (VSC) based HVDC is known as VSC-HVDC, which has the ability to reverse the direction of power flow by reversing the DC current but without reversing the DC voltage polarity [9]. Figure 2.2 shows an HVDC system based on VSC technology.

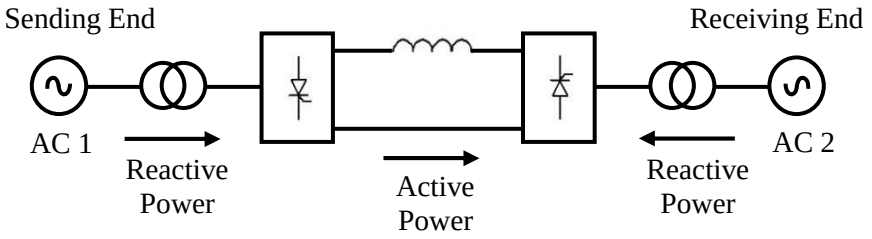

Figure 2.1. HVDC System Based on CSC Technology with Thyristors

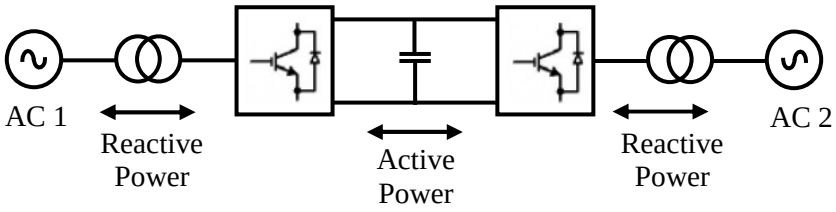

Figure 2.2. HVDC System Based on VSC Technology with IGBTs

Many HVDC projects have been implemented and several others are currently under construction. Table 2.1 shows the major HVDC projects that have been built between 1954 and 2011 [8]. In addition, Table 2.1 shows how the voltage levels of HVDC projects have increased over the same time period. This reflects the growing demands of electrical power and the development of HVDC systems over the years.

Table 2.1. Major HVDC Projects from 1954 to 2011

Project Name	*Location*	*Year*	*System Details*		
			MW	*kV*	*km*
Gotland	Sweden	1954	20	±100	96
Volgograd-Donbass	Russia	1962	720	±400	473
N. Z. Inter-Island	N. Zealand	1965	600	±250	609
Sardinia	Italy	1967	200	200	413
Pacific Intertie	USA	1970	1440	±400	1362
Nelson River	Canada	1973	1854	±463	890
Cahora-Bassa	MZ-ZA	1975	1920	±533	1456
Hokkaido-Honshu	Japan	1979	300	250	167
Itaipu	Brazil	1986	3150	±600	785
Quebec-N. England	Canada-USA	1990	2250	±450	1500
Directlink	Australia	2000	180	±80	59
East-South Intercon.	India	2003	2000	±500	1450
Celilo	USA	2004	3100	±400	1200
Norned	NO-NL	2008	700	±450	580
Yunnan-Guangdong	China	2010	5000	±800	1418
Xiangjiaba-Shanghai	China	2011	6400	800	2071

2.2. COMPARISON OF CONVENTIONAL HVDC AND VSC-HVDC

HVDC technology provides a good solution for transmitting electric power over long distances. Today, there are two types of HVDC systems: conventional HVDC and VSC-HVDC. Conventional HVDC is characterized by uni-directional DC current flow and the direction of active power flow is determined by DC voltage polarity. In contrast to conventional HVDC systems, VSC-HVDC systems can reverse the active and reactive

power flow by reversing the DC current and without reversing the DC voltage polarity. This makes the VSC-HVDC suitable for multi-terminal VSC-HVDC (M-VSC-HVDC) systems, as the DC voltage polarity will not change when the power flow is reversed for a single VSC. In M-VSC-HVDC systems, the individual transmission lines share a common DC voltage source and the power flow direction is determined by the current flow on the individual lines.

Another difference between conventional HVDC and VSC-HVDC is that conventional HVDC converters consume reactive power; therefore, they require a strong AC network for commutations. Since reactive power support is not required for VSC-HVDC, these systems may connect to a weak AC system. Table 2.2 presents a comparison of the conventional HVDC and VSC-HVDC [11].

Table 2.2. Comparison of Conventional HVDC and VSC-HVDC

Criteria	*Conventional HVDC*	*VSC-HVDC*
Commutation	Line-commutated	Self-commutated
Controllability	Controls active power only	Control active and reactive power independently
Power Direction Control	By the polarity of the DC voltage	By the polarity of the current
Reversal Capability	Limited power reversal capability	Fast response for reversing power flow
AC System	Requires a strong AC network	May connect to a weak AC grid
M-HVDC	Unsuitable for M-HVDC	Suitable for M-HVDC
Reactive Power Supply	Need reactive power supply	No need reactive power supply
Physical Size	Larger than VSC-HVDC	Smaller than conventional HVDC
Installation and Operation Time	Takes more time than VSC-HVDC	Takes less time than conventional HVDC

2.3. HVDC SYSTEM CONFIGURATIONS

HVDC systems have several configurations that can be identified to satisfy an effective function. The selection of the HVDC configuration depends on the function and location of the converter station [10].

2.3.1. Monopolar HVDC System. Figure 2.3 shows monopolar system consisting of two converters, which are separated by a single pole line and a positive or a negative DC voltage. The ground is used for the return current. A metallic return conductor may be used rather than using the ground as a return current [10].

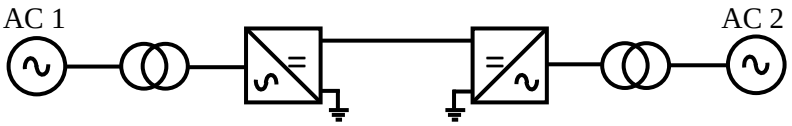

Figure 2.3. Monopolar HVDC System

2.3.2. Bipolar HVDC System. The bipolar HVDC configuration shown in Figure 2.4 consists of two monopolar systems to increase the power transfer capacity. Each system can operate as an independent system if both neutrals are grounded. Therefore, the system can continue to transmit power even in the case that the other line is out of service. The two lines are used as positive and negative poles, and in that case that both poles have equal currents, the ground current is theoretically zero [10].

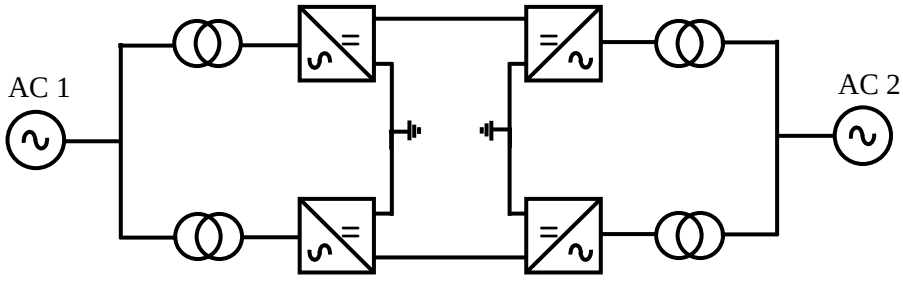

Figure 2.4. Bipolar HVDC System

2.3.3. Back-to-Back HVDC System. In Back-to-Back HVDC systems as shown in Figure 2.5, the two converter stations are built at the same location and there is no long distance transmission of power over the DC line. This type of configuration can be used to interconnect two AC systems with different frequencies (i.e. 60Hz and 50Hz) and/or non-synchronous systems [10]. Back-to-Back HVDC systems may also be used to interconnect two AC systems that experience difficulty synchronizing.

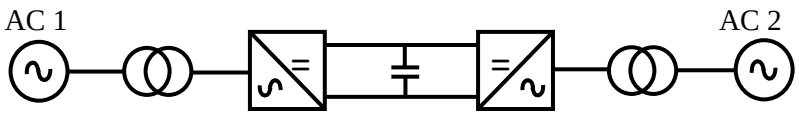

Figure 2.5. Back-to-Back HVDC System

2.3.4. Multi-terminal HVDC System (M-HVDC). M-HVDC systems connect more than two converters together providing additional reliability through the ability to compensate for the loss of any single converter of the system as shown in Figure 2.6. Typically, one of the converters regulates the DC voltage and the others converters control the power flow. This configuration will be discussed in greater detail throughout this thesis work.

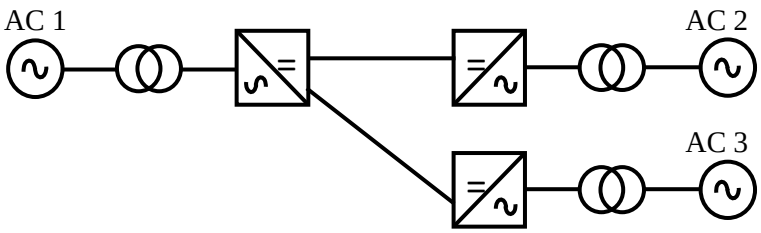

Figure 2.6. Multi-terminal HVDC System-Three Terminals

2.4. M-HVDC CHALLENGES

Although M-HVDC systems may provide more reliability and stability to the transmission system, there are some challenges that must be overcome.

2.4.1. Protection. DC circuit breakers are not yet commercially available for high power levels. Currently, the only way to clear a DC fault is to open the circuit breaker on the AC side. Furthermore, it is difficult to determine the fault location on the DC side within an M-HVDC. M-HVDC requires a very fast (within 1 *ms*) fault detection on the DC side fault and locating the DC side fault [12].

2.4.2. Power Flow Control. Typically, one of the converters within M-HVDC system controls the DC side voltage. The other converters independently control the power flow. With one converter controlling the DC voltage while the remaining converters controlling the active power flow, there is a danger of losing one or more converters because the DC voltage control converter assumes the entire power balance, thereby stressing the converter. This is particularly important challenge because the AC system connected to that particular converter will experience a large change [12] if any of the converters are suddenly lost.

3. MODELING OF M-VSC-HVDC

3.1. INTRODUCTION

The VSC is one of many devices that have been developed to make the high-voltage side of the network electronically controllable. This group of devices is called flexible ac transmission system (FACTS). Many operational problems in power systems have been solved using HVDC and FACTS devices. Although most of the existing HVDC installations are two terminal installations, it is possible to connect three or more terminals using voltage source converters (VSCs). Therefore, HVDC and FACTS devices may contribute more features to transmission of electrical power than in the case of using conventional AC transmission. Some of these features are:

- Power transmission over long distances
- Bi-directional power flow
- Fast response and accurate control of power flow
- Connecting two AC systems with different frequencies or without being synchronized

In contrast to the traditional thyristor HVDC system, the VSC-HVDC system has the following features [11]:

- Multi-terminal-HVDC systems have non-complex topologies
- A VSC-HVDC system has the ability to independently control active and reactive power flow or control the DC side voltage instead of the active power flow
- VSC-HVDC systems require lower cost for filtering of harmonics if suitable PWM techniques are used
- A VSC-HVDC system requires less time for installation and operation

3.2. VSC-HVDC SYSTEM

3.2.1. Configuration. Figure 3.1 shows the basic structure of a two level VSC-HVDC system. A two level VSC consists of a six-pulse bridge employed with semiconductors switches (IGBTs) and parallel diodes connected in the opposite direction to allow power to flow in either direction. The transformer is used to interconnect the VSC with the AC network with a voltage level suitable to the converter. The DC capacitor reduces the voltage ripple on the DC side. In addition, a filter can be used to isolate the harmonics due to switching of the IGBTs away from the AC system. The shunt capacitances, shunt resistances, and series inductances of the DC links are neglected. Only the series resistances are considered in the DC links for long distances. By using Pulse Width Modulation (PWM) techniques with high switching frequencies, the waveform of the converter AC voltage can be created to be almost sinusoidal. Thus, the phase angle and magnitude can be instantaneously adjusted by changing the PWM pattern. The ability to change either the phase angle or magnitude means that it is possible to control the active and reactive power flow independently.

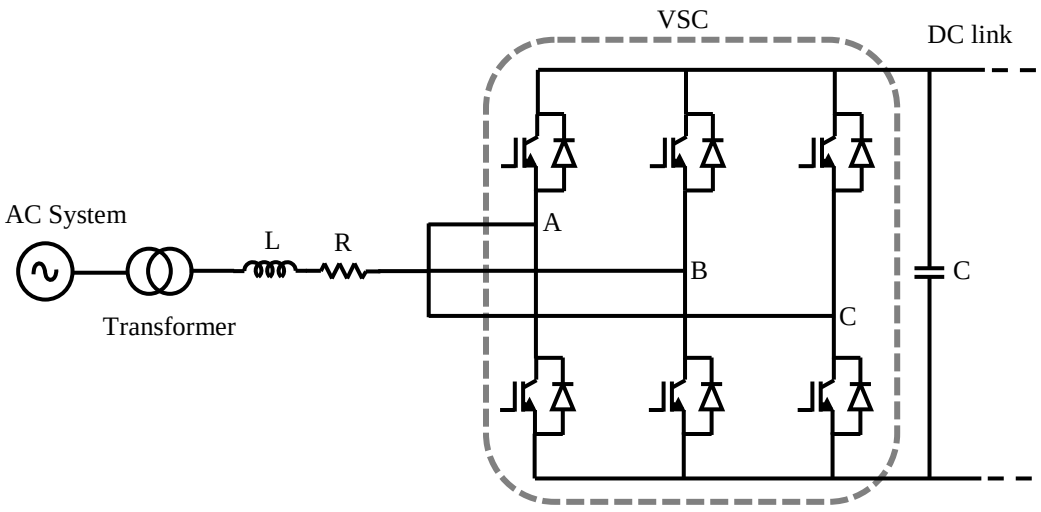

Figure 3.1. Basic Configuration of VSC-HVDC

3.2.2. PWM Techniques. The switches in the VSCs can be turned on or off as required by applying signals at the gate of IGBTs. There are several techniques used to generate these signals for VSCs such as sinusoidal PWM, optimized PWM, and space vector PWM. Sinusoidal PWM, which will be considered in this thesis, is the simplest technique. As shown in Figure 3.2, sinusoidal PWM generates the desired output voltage by comparing a high frequency triangular waveform "carrier" with the sinusoidal reference waveform. If the reference waveform magnitude is larger than the carrier magnitude, the switch is turned on. However, if the reference waveform magnitude is smaller than the carrier magnitude, the switch is turned off.

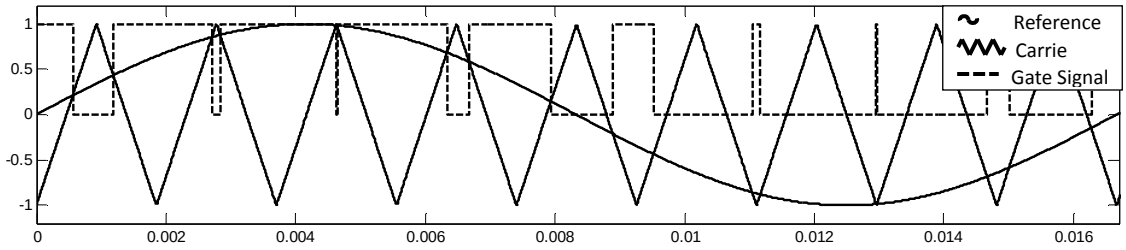

Figure 3.2. Sinusoidal PWM Pattern

3.3. MULTI-TERMINAL-VSC-HVDC SYSTEMS

Multi-terminal-VSC-HVDC (M-VSC-HVDC) links connect together two or more converters providing additional reliability through the ability to compensate for the loss of any single converter of the system [7]. A three terminal VSC-HVDC system is illustrated in Figure 3.3.

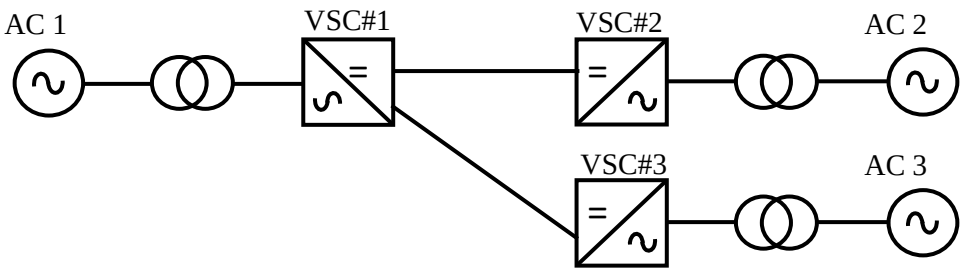

Figure 3.3. Three-terminal VSC-HVDC Configuration

3.3.1. Operating and Control Principles of M-VSC-HVDC. Figure 3.3 shows a M-VSC-HVDC system consisting of three converters VSC#1, VSC#2, and VSC#3,

which are directly connected with a DC link. VSC#1 provides the DC side voltage control and power exchange balance among the converters. VSC#2 and VSC#3 provide active power flow control. The steady state power flow can be controlled in either direction at VSC#2 and VSC#3. Consequently, both VSC#2 and VSC#3 can operate in either rectifier or inverter mode. The general control approach will be made for one VSC and will be used for all the others VSC-HVDC terminals throughout this thesis work. However, different control strategies will be employed depending on the required control of each converter either power flow control or DC voltage control as shown in Figure 3.4.

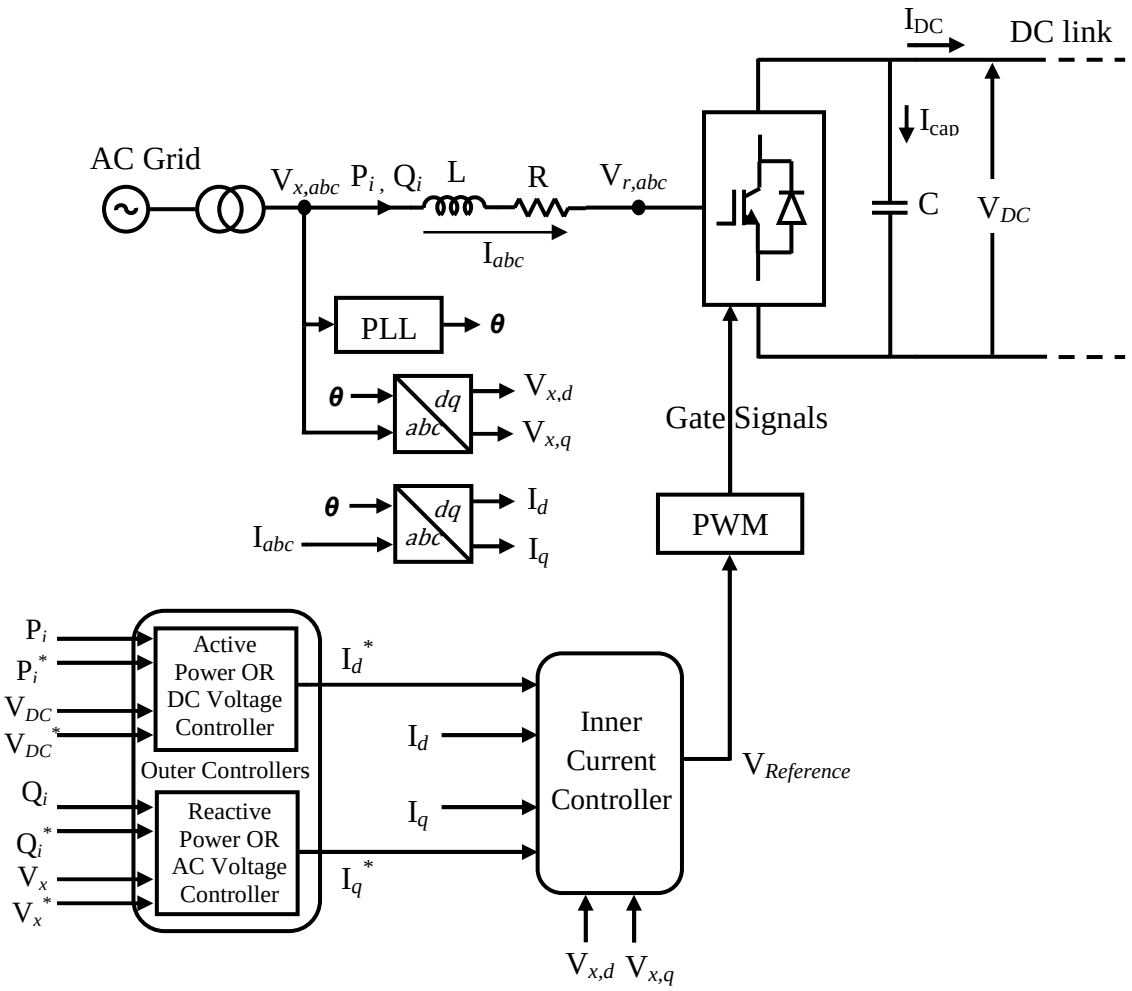

Figure 3.4. Simplified Circuit Diagram of VSC-HVDC Controllers

The inner current controller, which is always equipped with a phase lock loop (PLL) to determine the phase angle and frequency instantaneously, is the fundamental part of the VSC control. The inner current controller depends on the synchronously rotating reference frame for observing all the AC voltage and current quantities involved in the VSCs.

3.4. CONTROL STRATEGY

In this section, controls for different modes of VSC-HVDC system will be discussed. The vector control method will be used to make the active and reactive current linear. Hence, static errors in the control system can be avoided by using PI controllers. The basic structure of VSC-HVDC system control is shown in Figure 3.4.

3.4.1. Vector Control. Different control strategies have been developed for the control of VSC-HVDC. One of the methods for control of VSC-HVDC is known as the vector control method, which is transforming a three-phase system into a two-phase system by using *dq*-axis transformations. As shown in Figure 3.5, vector control works by transferring the vectors of AC currents and voltages to two-phase constant vectors in steady state and therefore static errors in the control system can be avoided by using PI controllers. Thus, vector control systems can be used to obtain independent control of the active and reactive powers.

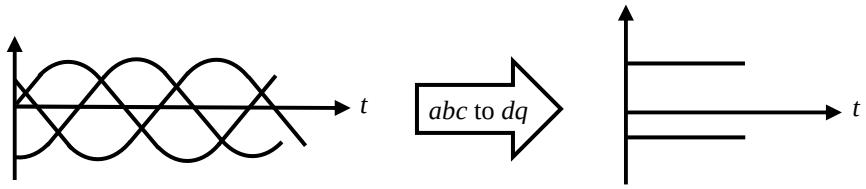

Figure 3.5. DQ-axis Transformation Principle

For analysis of the VSC-HVDC, considering the converter system connected to AC network and the currents I_{abc}, are injected to the converter. The AC network voltages are defined as $V_{x,\,abc}$, and the converter input voltages $V_{r,\,abc}$, and resistance (R) and inductance (L) between the converter and the AC network, as shown in the system of Figure 3.4. The voltage at the AC network side of the converter can be expressed as:

$$V_{x,abc} = RI_{abc} + L\frac{dI_{abc}}{dt} + V_{r,abc} \qquad (3.1)$$

Applying the *dq* transformation equation (3.1) yields:

$$\frac{di_d}{dt} = \frac{v_{x,d} - v_{r,d}}{L} - \frac{R}{L} i_d + \omega\, i_q \qquad (3.2)$$

$$\frac{di_q}{dt} = \frac{v_{x,q} - v_{r,q}}{L} - \frac{R}{L} i_q - \omega\, i_d \qquad (3.3)$$

where ω is frequency of the fundamental component in the AC network.

The active power injected into or absorbed from the AC network is given by:

$$P_i = \frac{3}{2}(v_{x,d} i_d + v_{x,q} i_q) \qquad (3.4)$$

3.4.2. Inner Current Controllers. An inner current controller is developed based on equations (3.2) and (3.3) as shown in Figure 3.6. I_d^* and I_q^* are reference currents for the *d*-axis and *q*-axis current controllers respectively.

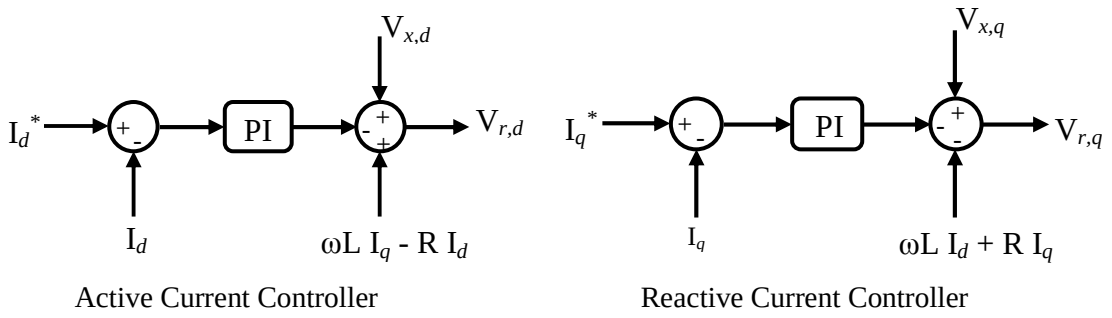

Figure 3.6. Inner Current Controllers

$V_{r,d}$ and $V_{r,q}$ are the *dq* reference frame voltages which are transferred to the *abc* frame and $V_{r,abc}$. $V_{r,abc}$ are the reference voltages for the PWM.

3.4.3. Outer Controllers. The active current reference I_d^* can be used to control either the active power flow or the DC voltage level as will be illustrated in the next section.

3.4.3.1 Active power control. The *dq* reference frame is selected in a direction such that the *d*-axis is in phase with the AC source voltage. This means that

$$v_{x,q} = 0$$

Therefore, equation (3.4) can be rewritten as

$$P_i = \frac{3}{2} v_{x,d} i_d \qquad (3.5)$$

Equation (3.5) implies that the active power flow can be controlled by the active current i_d. Therefore, the output of the active power controller will be the reference input to the active current controller I_d^* of the inner current controllers in Figure 3.6. The active power controller is shown in Figure 3.7. P_i^* is a reference active power flow.

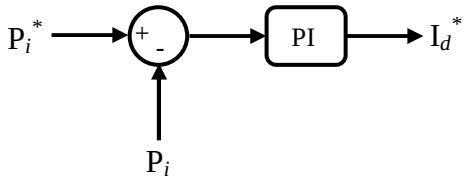

Figure 3.7. Active Power Controller

3.4.3.2 DC voltage control. From the active power balance of the VSC-HVDC in Figure 3.4, the relation can be as following (ignoring the converter losses):

$$P_i = P_{DC} + P_{cap} \quad (3.6)$$

where P_i refers to the power transferred from the AC source toward the DC lines, and P_{DC} and P_{cap} refer to the power flowing into the DC lines and the DC capacitor respectively.

$$P_{DC} = V_{DC} I_{DC} \quad (3.7)$$

$$P_{cap} = V_{DC} I_{cap} \quad (3.8)$$

$$I_{cap} = C \frac{dV_{DC}}{dt} \quad (3.9)$$

From equations (3.5), (3.6), (3.7), (3.8) and (3.9), the differential equation for the DC voltage is:

$$C \frac{dV_{DC}}{dt} = \frac{3 v_{x,d} i_d}{2 V_{DC}} - I_{DC} \quad (3.10)$$

Equation (3.10) indicates that the DC voltage can be controlled by the active current i_d. Although the I_{DC} in equation (3.10) can be represented as a feed forward control in the DC voltage controller, the DC voltage can be controlled without a feed

forward control loop because the PI controller has the ability to maintain the DC voltage constant. Thus, the DC voltage controller will be as shown in Figure 3.8.

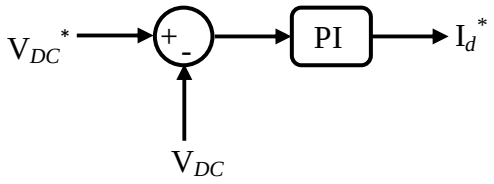

Figure 3.8. DC Voltage Controller

Figure 3.9 shows the active power output of VSC#2 for a commanded output of 200 MW. At 3.0 seconds, the commanded output reference signal is changed to 300 MW. Although the active power output of VSC#2 readily tracks the commanded reference signal, the DC link voltage remains nearly constant throughout the change in active power as shown in Figure 3.10.

Figure 3.11 shows the active current of the VSC#2 and the active current reference signal. In Figure 3.12, the output of the active power controller will be the reference input to the active current controller I_d^* of the inner current controllers in Figure 3.13.

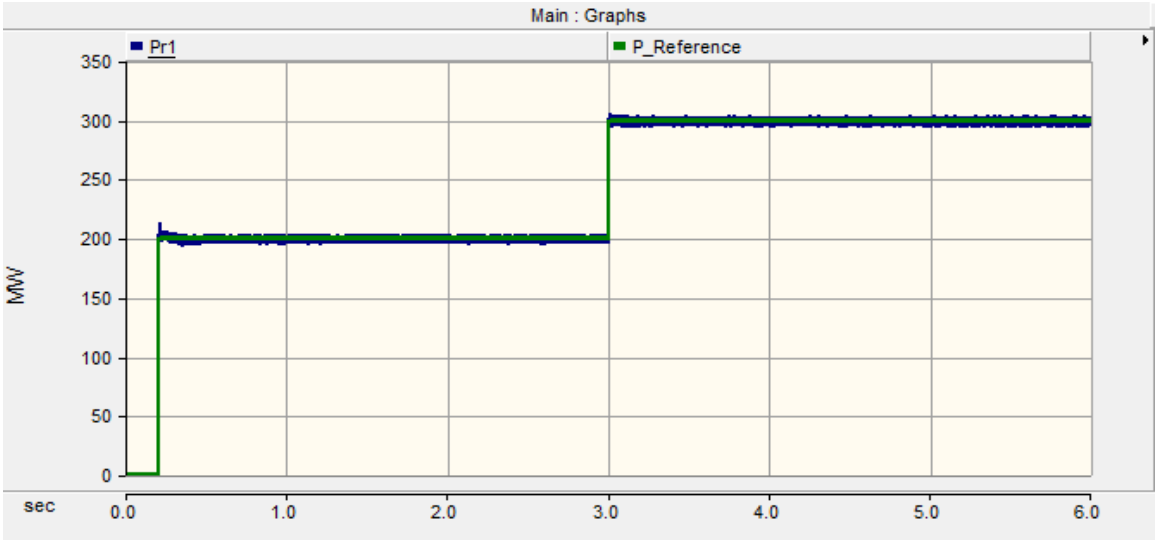

Figure 3.9. Active Power Flow Control With 200 MW and 300 MW as Reference Signals

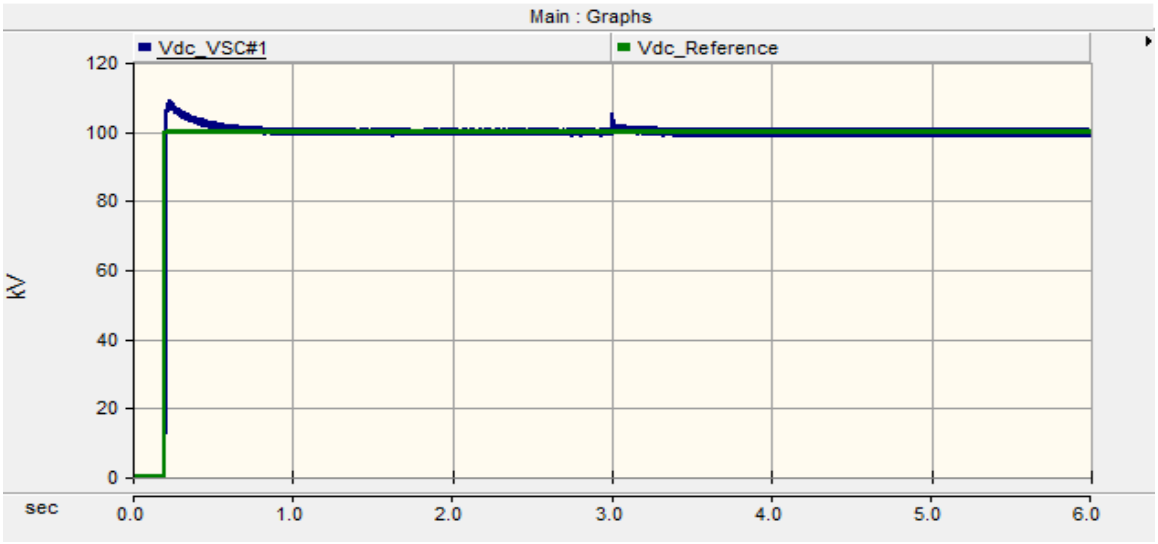

Figure 3.10. DC Voltage Control With 100 kV as Reference Signal

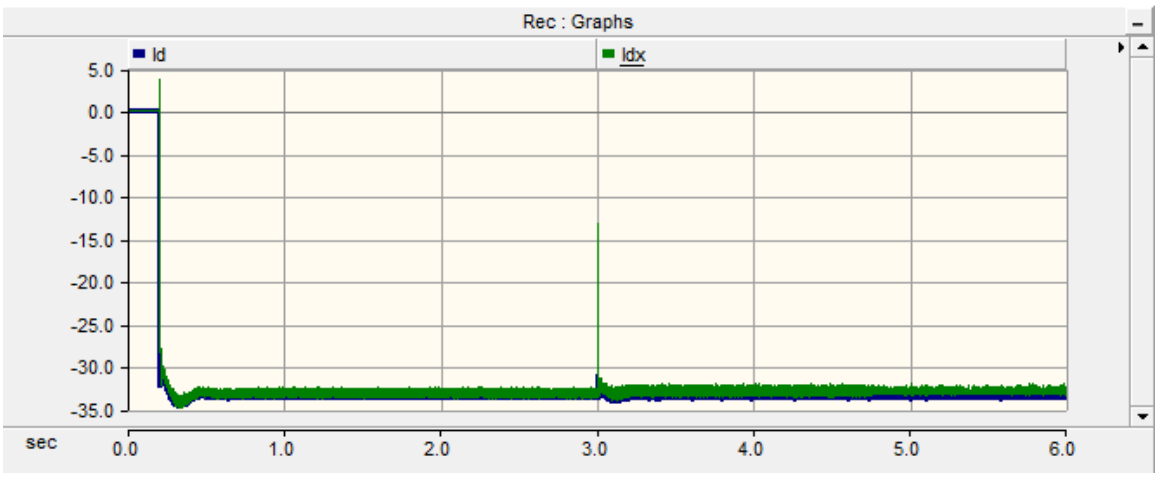

Figure 3.11. Active Current and Active Current Reference Signal

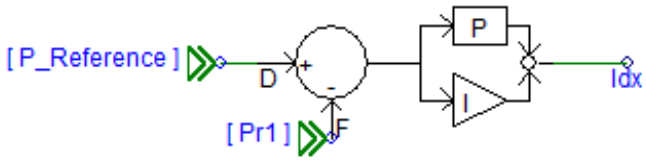

Figure 3.12. Active Power Controller

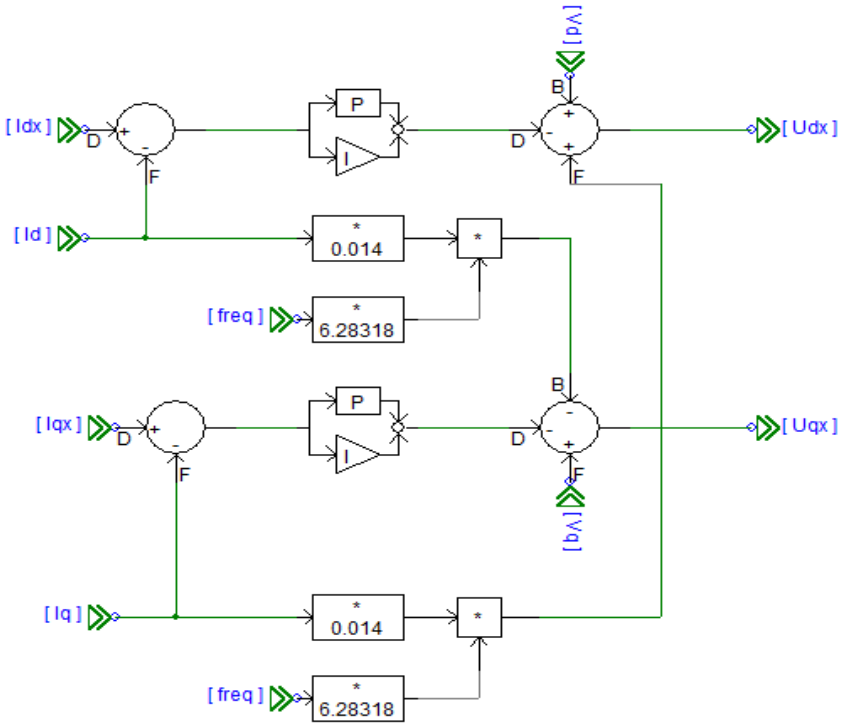

Figure 3.13. Inner Current Controller of Simulation

4. SYSTEM STUDY AND SIMULATION RESULTS

4.1. SYSTEM DESCRIPTION

The interconnection of three AC grids through a voltage source converter based M-HVDC system was simulated in PSCAD/EMTDC. The simulation was designed to illustrate the bulk power transfer over the DC link while achieving an independent control over active power and DC voltage. In addition, the region of controllability as a function of power flow will be analyzed. Furthermore, the steady-state and dynamic response characteristics as a function of capacitor size will be investigated.

Controlling the DC voltage inside a M-HVDC transmission system is very important because a constant DC voltage on a M-HVDC transmission network will allow the active power to be distributed among the converters. Typically, the control of a M-HVDC transmission system is obtained as follows: one converter controls the DC voltage while the other converters control the active power flow.

The three-terminal VSC-HVDC network shown in Figure 4.1 was implemented in PSCAD/EMTDC. The control of this model is organized as follows: VSC#1 is used to control the DC voltage, whereas VSC#2 and VSC#3 are used to control the active power in either direction independently. The line impedances data for the AC network are presented in Table 4.1 (MVA base for all the AC system is 100MVA). Table 4.2 presents the load flow data for the system.

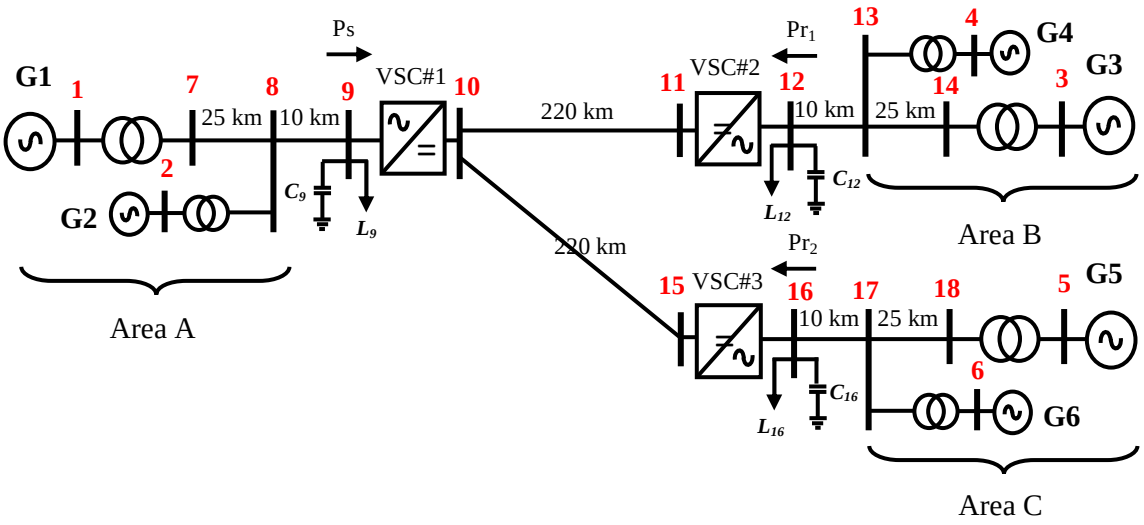

Figure 4.1. Multi-terminal HVDC System

Table 4.1. Lines Impedance Data for the Three-terminal HVDC System

From Bus	*To Bus*	*R (pu)*	*X (pu)*	*B (pu)*
1	7	0	0.15	0
2	8	0	0.15	0
3	14	0	0.15	0
4	13	0	0.15	0
5	18	0	0.15	0
6	17	0	0.15	0
7	8	0.0025	0.025	0.04375
8	9	0.001	0.01	0.0175
12	13	0.001	0.01	0.0175
13	14	0.0025	0.025	0.04375
16	17	0.001	0.01	0.0175
17	18	0.0025	0.025	0.04375

The VSC-HVDC lines data (on Base V_{DC}=100 kV and 400 MW) are:

R_{DC} =0.55 Ω C_{DC} =800 μF

All the transformers in the system have the same parameters as follows:

Base, 900 MVA, 20 kV/230 kV, 15%

The generators' dynamic data for the three-terminal HVDC system are:

Base, 900 MVA, 20 kV, 60 Hz

$X_d = 1.8\ pu$ $X'_d = 0.3\ pu$ $X''_d = 0.25\ pu$ $X_q = 1.7\ pu$ $X'_q = 0.55\ pu$

$X''_q = 0.25\ pu$ $T'_{d0} = 8\ s$ $T''_{d0} = 0.03\ pu$ $T'_{q0} = 0.4\ pu$ $T''_{q0} = 0.05\ s$

$R_a = 0.0025\ pu$ $H = 6.5\ (For\ G1\ and\ G2)$ $H = 6.175\ (For\ G3, G4, G5\ and\ G6)$

Table 4.2. Load Flow Data for the Three-terminal HVDC System

Bus	*V (pu)*	*θ (°)*	*P_L (MW)*	*Q_L (MVAR)*	*Q_C (MVAR)*
1	1.03	20.2	-	-	-
2	1.01	10.5	-	-	-
3	1.03	-6.80	-	-	-
4	1.01	-17.0	-	-	-
5	1.03	-6.80	-	-	-
6	1.01	-17.0	-	-	-
9	-	-	967	100	9971
12	-	-	1767	100	9971
16	-	-	1767	100	9971

4.2. ACTIVE POWER CONTROL STUDIES

The M-HVDC system has been studied and simulated at different operating conditions to analyze and observe the active power transmission over the DC link. The region of controllability as a function of power flow will be determined. Furthermore, the steady-state and dynamic response characteristics as a function of capacitor size will be investigated.

4.2.1. Normal Operation. The system has to be examined under normal condition to verify that it is working properly. VSC#1 maintains the DC voltage at 100 kV as shown in Figure 4.2, and the other converters control the active power as needed. Table 4.3 and Figure 4.3 show that the active power (P_{r1} and P_{r2}) can be independently controlled in either direction under normal operating conditions. Note that

$$P_s = -(P_{r1} + P_{r2})$$

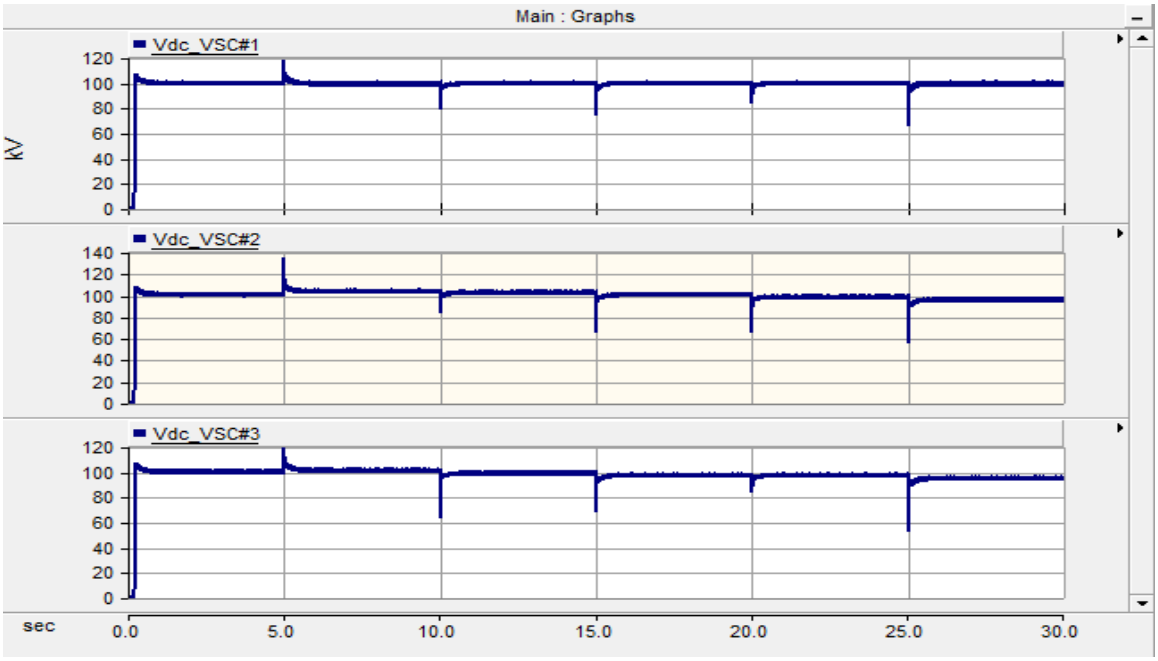

Figure 4.2. DC Voltage of the Normal Operation for the Three-terminal HVDC

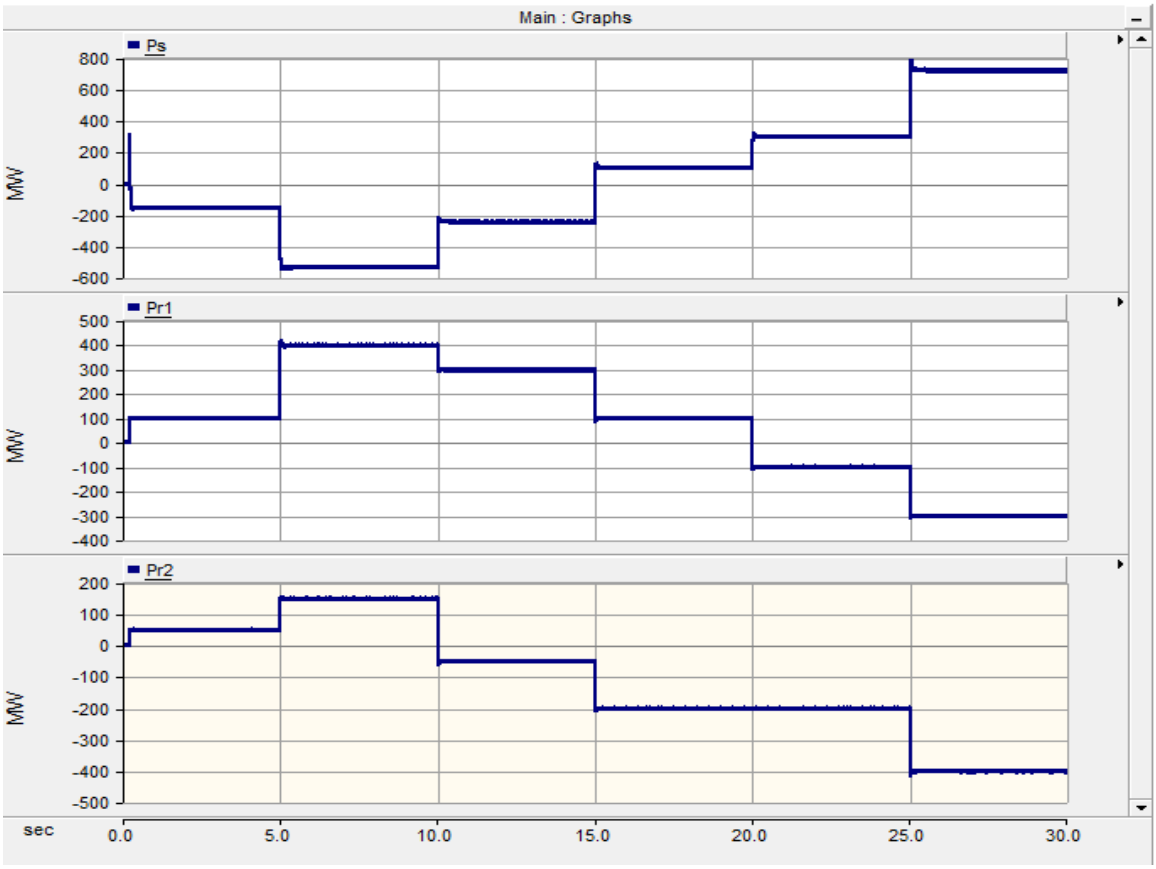

Figure 4.3. Power Flow of Normal Operation for the Three-terminal HVDC

Table 4.3. Series of Test Scenarios for Normal Operation

Time (s)		*Ps*	*Pr_1*	*Pr_2*	*P_{G1}*	*P_{G2}*	*P_{G3}*	*P_{G4}*	*P_{G5}*	*P_{G6}*
From	*To*	*(MW)*	*(MW)*	*(MW)*	*(MW)*	*(MW)*	*(MW)*	*(MW)*	*(MW)*	*(MW)*
0	*5*	*-140*	*100*	*50*	*530*	*270*	*870*	*1070*	*845*	*1010*
5	*10*	*-520*	*400*	*150*	*425*	*10*	*1010*	*1420*	*895*	*1130*
10	*15*	*-230*	*300*	*-50*	*505*	*210*	*965*	*1305*	*795*	*890*
15	*20*	*114*	*100*	*-200*	*595*	*440*	*870*	*1070*	*715*	*700*
20	*25*	*314*	*-100*	*-200*	*650*	*570*	*770*	*830*	*715*	*700*
25	*30*	*740*	*-300*	*-400*	*750*	*860*	*666*	*585*	*613*	*460*

4.2.2. Region of Controllability. The operating boundaries of controllability as a function of power flow are important to determine the converter rating power flow. Hence, the region of controllability ensures that the system is stable as long as the converter rating power is considered. The operating boundaries of controllability can be investigated using a series of test scenarios by changing the specified power flows P_{r1} and P_{r2} as shown in Table 4.4. The DC voltage is specified at 100 kV for all scenarios. For example, P_{r1} is specified at -400 MW while P_{r2} is increased in 200 MW steps until it reaches its peak value of 2200 MW as illustrated in Figure 4.4. In another scenario, P_{r1} is specified at 1200 MW while P_{r2} is increased in 200 MW steps until it reaches to 2000 MW as illustrated in Figure 4.5. Therefore, the maximum power of the converter VSC#1 flows to the AC grid is -2765 MW. Note that the negative sign means that the active power flows from the DC link to the AC network.

Because of the similarity between area *B* and area *C*, both areas have the same operating boundaries. From Figure 4.6, area *A* can provide up to 1565 MW to the DC link ($Ps_{,max}$), and each of area *B* and *C* can provide up to 2200 MW to the DC link ($Pr_{1,max}$ and $Pr_{2,max}$). Note that Pr_1 and Pr_2 obviously cannot both be 2200 MW simultaneously because *Ps* is limited to -2765 MW. Under normal operation, the total power losses in the DC links are relatively small, and therefore neglected. However, the power losses cannot be ignored if the system operates near the region of controllability limit because the losses in the DC links then become relatively large. (More cases are provided in Appendix A)

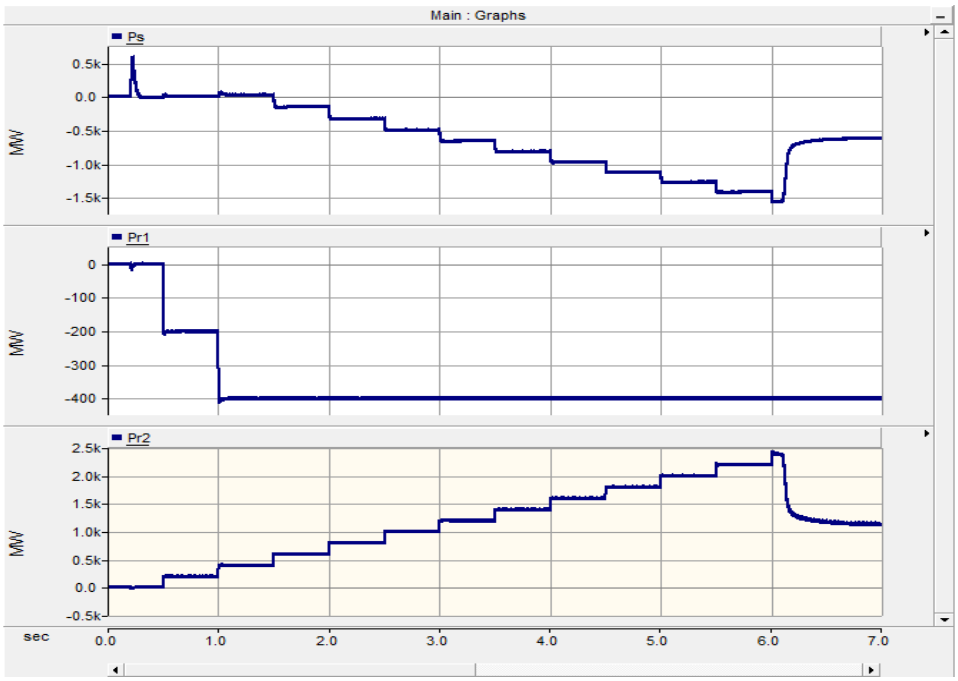

Figure 4.4. Increasing the Active Power Flow of VSC#2 (P_{r1}) to Peak Value

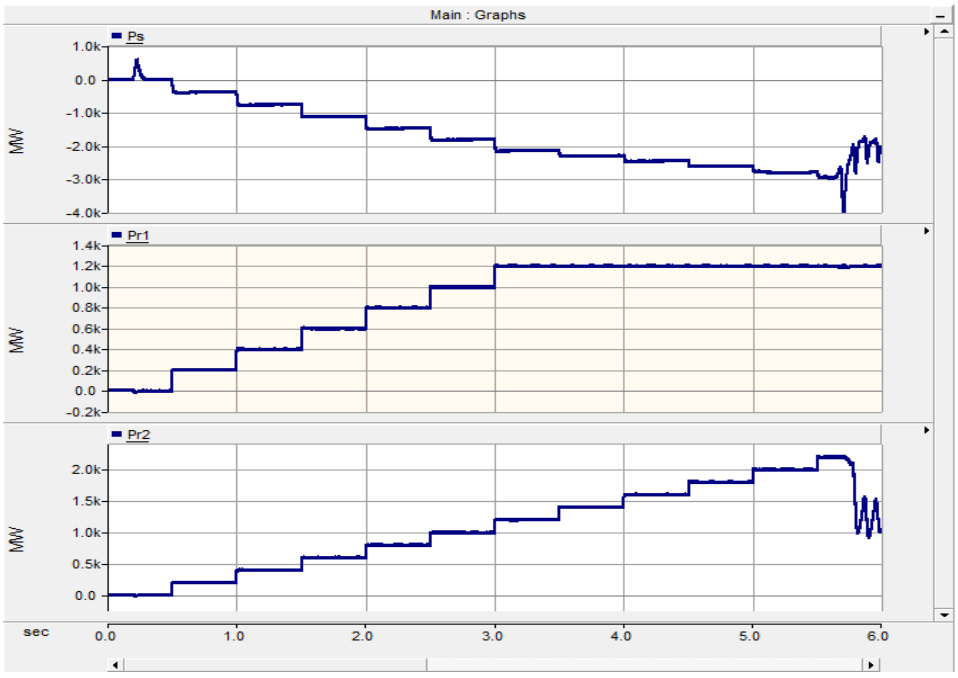

Figure 4.5. Decreasing the Active Power Flow of VSC#2 (P_{r2}) to Minimum Value

As seen in Figure 4.6, Pr1+Pr2+Ps≠0 near the region of controllability limit due to the power losses in the DC links. The power losses (I^2R) at some points are relatively high, and hence the efficiency is low. In this system, the DC links are specified at 100 kV. This voltage level may result in relatively high currents if high power (e.g. 1600 MW) transfers with the HVDC links. Thus, transmitting with high current over long distances with HVDC will result in extensive power losses. For instance, the active power P_{r1} and P_{r2} are specified at 1000 MW and 1400 MW respectively, and therefore Ps=-2125 MW and the losses is 275 MW. The efficiency in this case is 88.54%. However, the efficiency can be improved by increasing the DC voltage level. For example, the efficiency has been improved to 96.46% at the same specified power in the last example with V_{DC}=200 kV.

Figure 4.7 and Figure 4.8 show the HVDC power flow efficiency at 100 kV and 200 kV respectively. There are few cases in which the active power flow reaches nearly an efficiency of 100% with V_{DC}=100 kV as illustrated in Figure 4.7. However, Many cases come close to efficiency of 100% with V_{DC}=200 kV. Therefore, the efficiency can be improved by increasing the DC voltage to higher level.

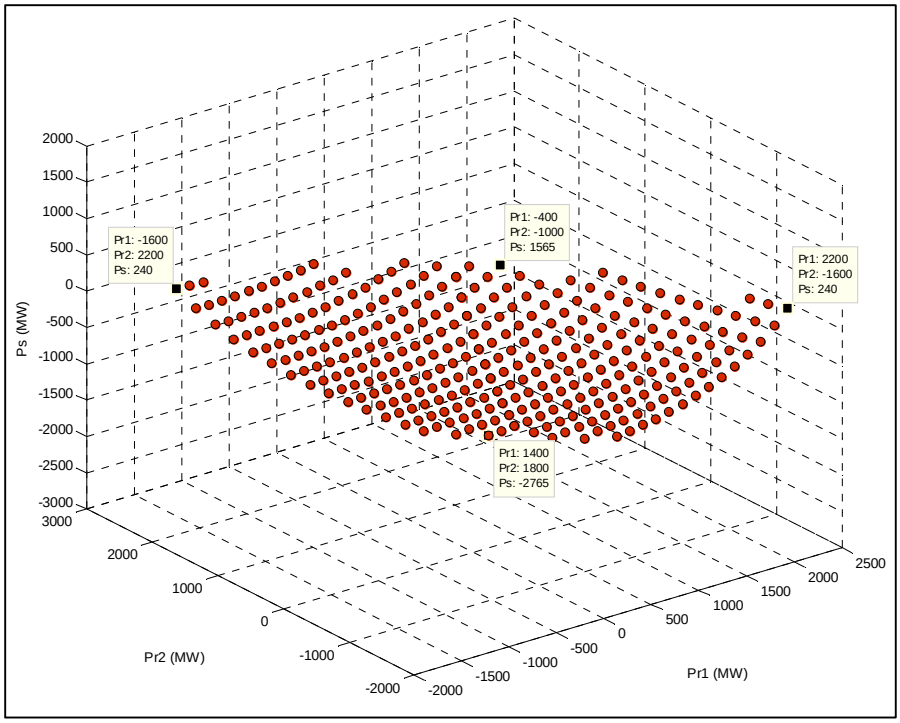

Figure 4.6. Three-Dimensional Region of Controllability

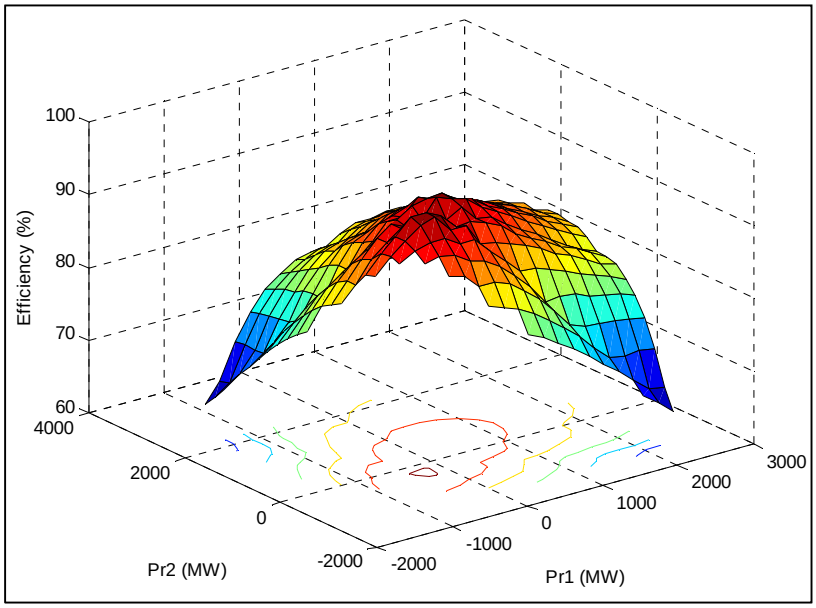

Figure 4.7. Three-Dimensional of Efficiency at V_{DC}=100 kV

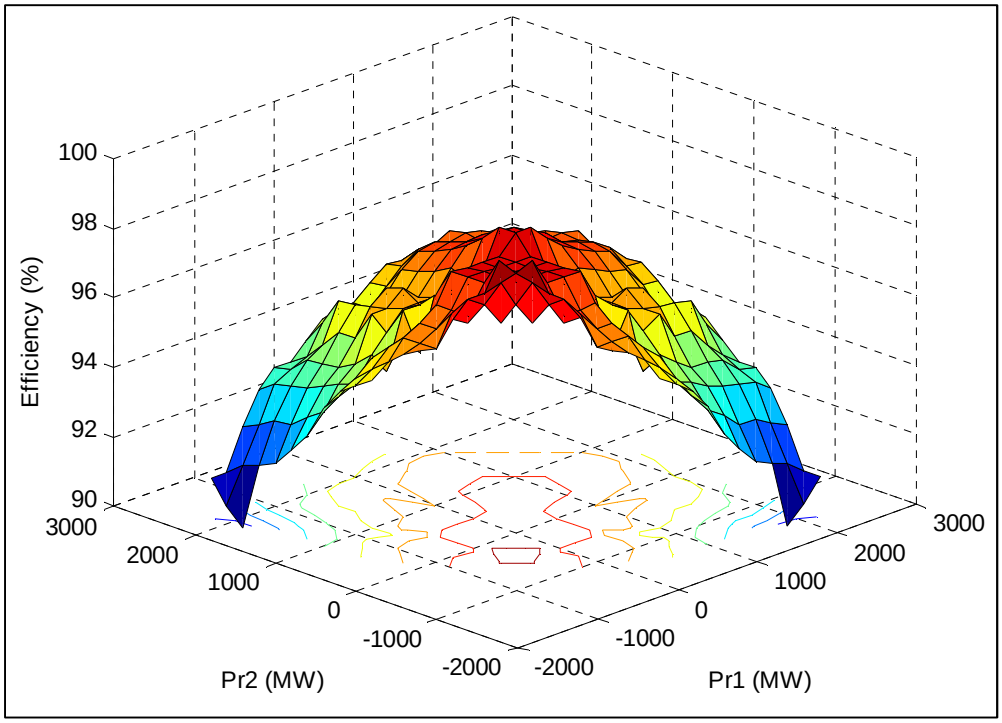

Figure 4.8. Three-Dimensional of Efficiency at V_{DC}=200 kV

Table 4.4. Series of Test Scenarios for Operating Boundaries Investigation

Pr_1	Pr_2	Ps
-1600	*1800*	*525*
-1600	*2000*	*380*
-1600	*2200*	*240*
-1400	*400*	*1340*
-1400	*600*	*1160*
⋮	⋮	⋮
-1000	*-400*	*1565*
-1000	*-200*	*1350*
⋮	⋮	⋮
1200	*1800*	*-2600*
1200	*2000*	*-2765*
1400	*1400*	*-2450*
1400	*1600*	*-2608*
1400	*1800*	*-2765*

4.2.3. Capacitor Size Effect. The size of DC side capacitor is an important part for the HVDC systems because the current flows to the DC side of the converter containing harmonics, which will result in a ripple on the DC side voltage. The magnitude of the ripple voltage depends on the DC side capacitor size. In this section, the level of controllability as the DC capacitor size is decreased will be investigated, and how different values impact the speed of response and the dynamic performance at M-HVDC.

4.2.3.1 Case#1. In this case, the DC capacitor size is 800 μF, which is the capacitor size used in all of the previous results. As seen in Figure 4.9, the active power controller has a fast response for a step change in the input reference. Furthermore, the

DC voltage has almost no ripple because the capacitor size is relatively large. However, the active power controller has a time delay and overshoot as shown in Figure 4.9.

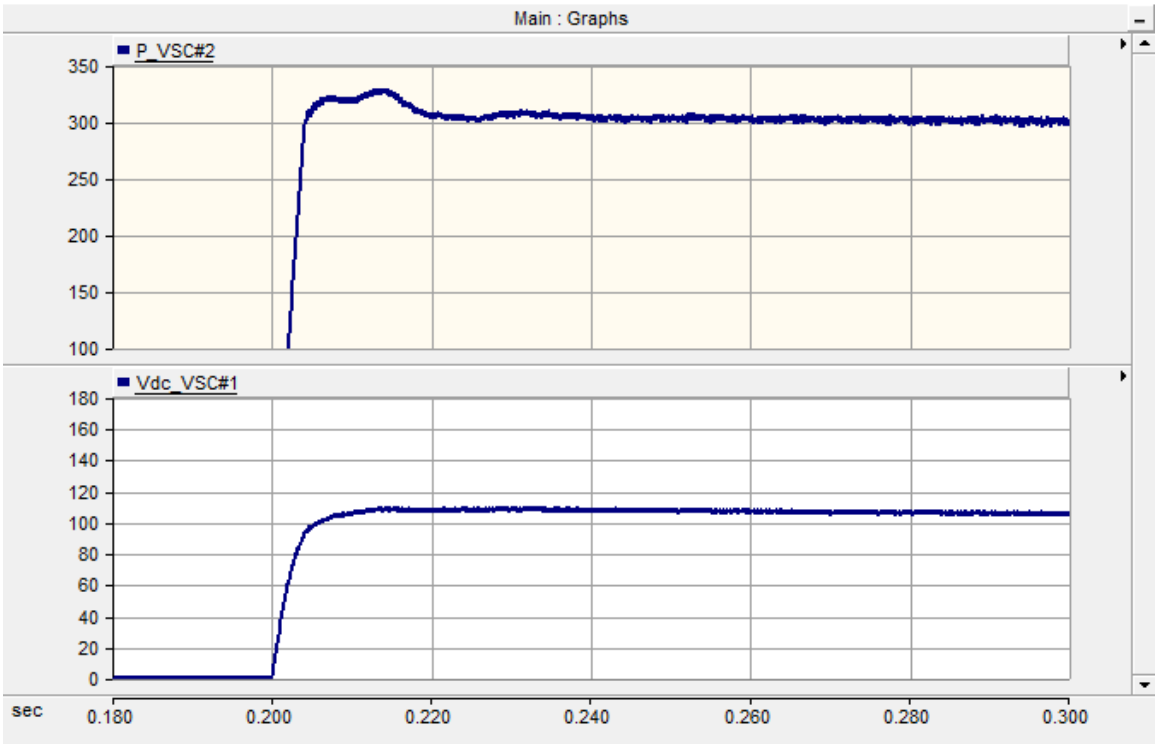

Figure 4.9. Active Power and DC Voltage Step Response at Capacitor Size of 800 µF

4.2.3.2 Case#2. In this case, the DC capacitor size has been decreased to 20 µF. The active power controller response has improved because the response has less time delay and overshoot as shown in Figure 4.10. However, there is a limitation in choosing a smaller size of capacitor as it will affect the dynamic operation of the HVDC system.

Thus, a smaller size of capacitor means high ripple voltage at the DC side as shown in Figure 4.10. (More cases are provided in Appendix B)

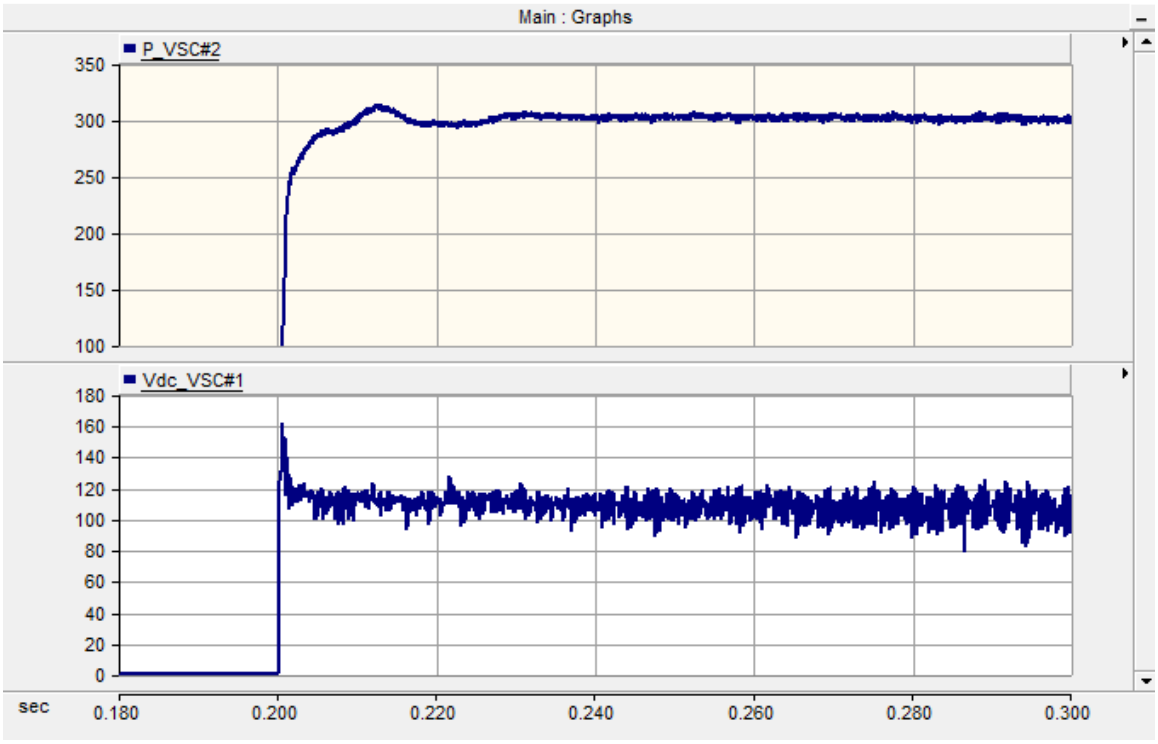

Figure 4.10. Active Power and DC Voltage Step Response at Capacitor Size of 20 μF

The design of DC side capacitor is an important part for the design of HVDC systems because the use of PWM in VSC results in current harmonics occurring in the DC side of the VSC-HVDC. These current harmonics cause ripple on the DC side voltage. The use of DC capacitor results in smoother DC voltage. However, the DC capacitor size should be designed based on the formula

$$\tau = \frac{1}{2} C \frac{V_{dc}^2}{S_n}$$

where S_n is the nominal power, V_{dc} is the DC voltage and τ is the time constant, which is equal to the time needed to charge the capacitor from zero to rated voltage. A smaller time constant means faster response and higher ripple voltage. In contrast, a larger time constant provides slower response and smaller ripple voltage. Thus, the time constant is suggested to be between 5 *ms* and 10 *ms*.

In case#2, the DC voltage cannot remain at the target value with a capacitor of 20 μF because the time constant τ is 0.25 *ms*, which is too small. However, the DC voltage has almost no ripple with a capacitor of 800 μF because the time constant is 10 *ms*, which is relatively good.

5. CONCLUSIONS

A model of a three-terminal VSC-HVDC system is presented in this thesis. The vector control strategy is described and implemented in PSCAD/EMTDC. The simulation results has shown that operation of M-VSC-HVDC is possible with one VSC terminal regulating the DC voltage while the others converters control the active power flow independently and bi-directionally. The region of controllability as a function of power flow is a very important from the stability point of view. The region of controllability is the region of stability. Hence, the region of controllability ensure that the system is stable as long as the converter rating power is considered. Furthermore, the steady-state and dynamic response characteristics as a function of capacitor size has been investigated. From the simulation results, it is concluded that the active power controller has a fast response for a step change in the input reference, and the DC voltage has almost no ripple if the capacitor size is relatively large. However, the active power controller response is improved when the capacitor size is decreased. Although a smaller capacitor size provides faster response, there is a limitation in choosing a smaller size of capacitor as it will affect the dynamic operation of the HVDC system. Thus, a smaller size of capacitor means high ripple voltage at the DC side.

APPENDIX A.
REGION OF CONTROLLABILITY TEST SCENARIOS

This table shows test scenarios of region of controllability at V_{DC}=100 kV.

P_{r1} (MW)	P_{r2} (MW)	Ps (MW)	P_{Losses} (MW)
-1600	1800	525	725
-1600	2000	380	780
-1600	2200	240	840
-1400	400	1340	340
-1400	600	1160	360
-1400	800	990	390
-1400	1000	820	420
-1400	1200	660	460
-1400	1400	500	500
-1400	1600	344	544
-1400	1800	190	590
-1400	2000	40	640
-1400	2200	-100	700
-1200	200	1225	225
-1200	400	1040	240
-1200	600	860	260
-1200	800	685	285
-1200	1000	515	315
-1200	1200	350	350
-1200	1400	192	392
-1200	1600	35	435
-1200	1800	-115	485
-1200	2000	-265	535
-1200	2200	-405	595
-1000	-400	1565	165
-1000	-200	1350	150
-1000	0	1150	150

-1000	*200*	*950*	*150*
-1000	*400*	*760*	*160*
-1000	*600*	*580*	*180*
-1000	*800*	*405*	*205*
-1000	*1000*	*235*	*235*
-1000	*1200*	*75*	*275*
-1000	*1400*	*-86*	*314*
-1000	*1600*	*-240*	*360*
⋮	⋮	⋮	⋮
800	*1200*	*-1795*	*205*
800	*1400*	*-1955*	*245*
800	*1600*	*-2115*	*285*
800	*1800*	*-2265*	*335*
800	*2000*	*-2410*	*390*
800	*2200*	*-2560*	*440*
1000	*1000*	*-1800*	*200*
1000	*1200*	*-1965*	*235*
1000	*1400*	*-2125*	*275*
1000	*1600*	*-2280*	*320*
1000	*1800*	*-2430*	*370*
1000	*2000*	*-2575*	*425*
1000	*2200*	*-2730*	*470*
1200	*1200*	*-2130*	*270*
1200	*1400*	*-2290*	*310*
1200	*1600*	*-2445*	*355*
1200	*1800*	*-2600*	*400*
1200	*2000*	*-2760*	*440*
1400	*1400*	*-2450*	*350*
1400	*1600*	*-2608*	*392*
1400	*1800*	*-2765*	*435*

APPENDIX B.
DC CAPACITOR SIZE EFFECT

C_{DC} =400 µF

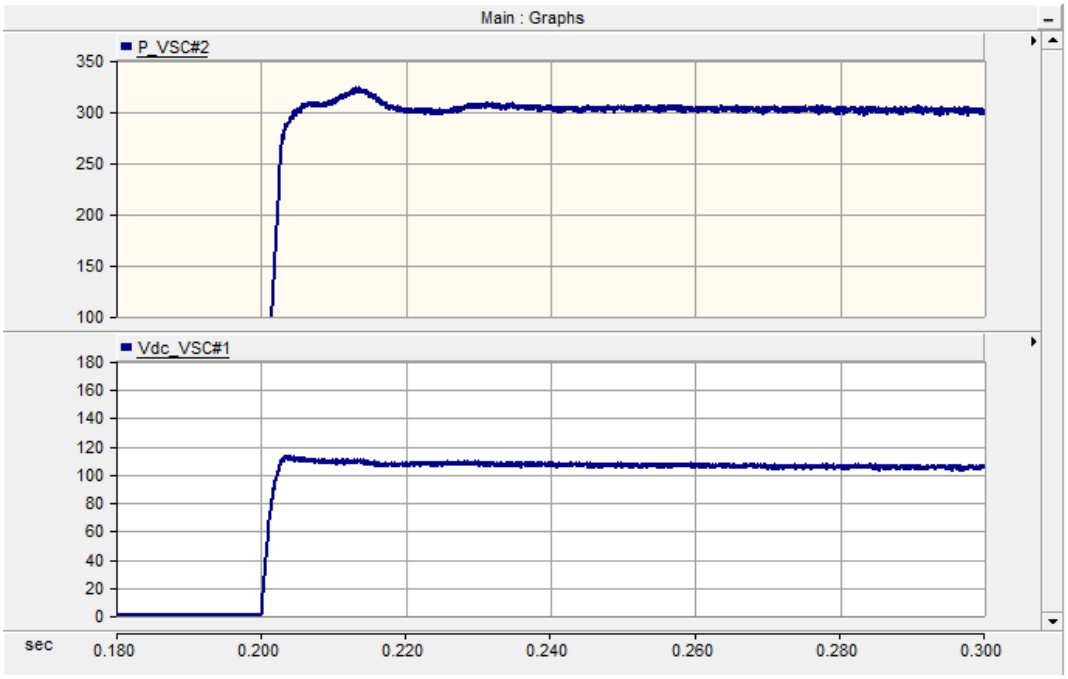

C_{DC} =100 µF

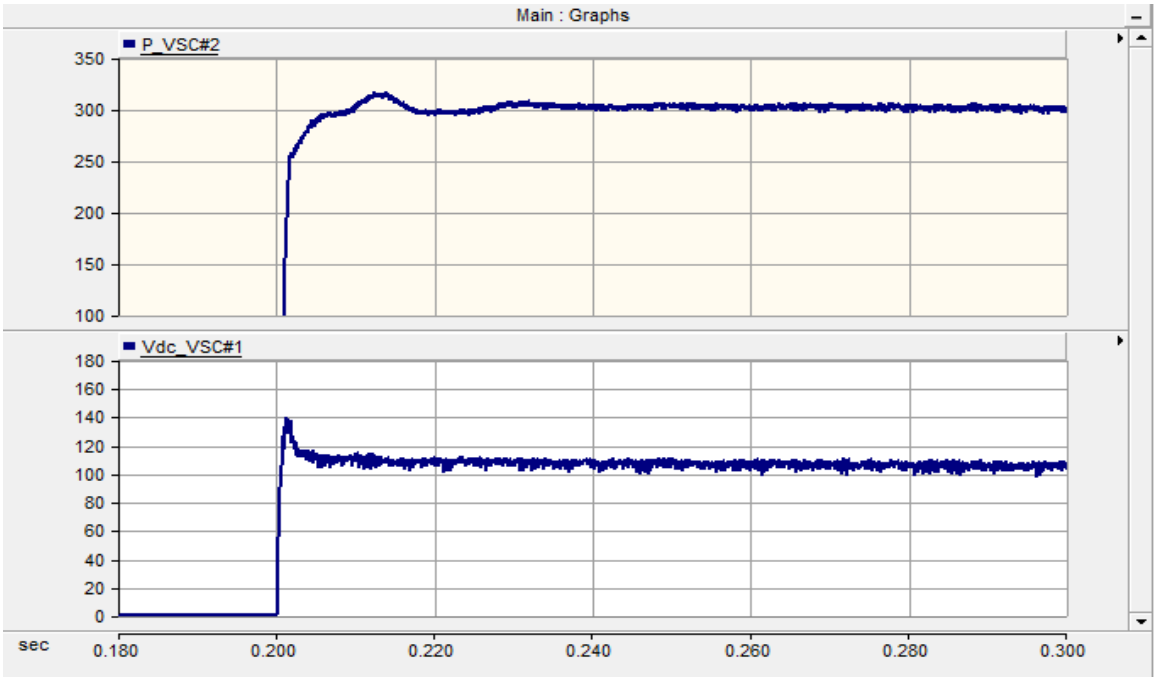

C_{DC} =40 µF

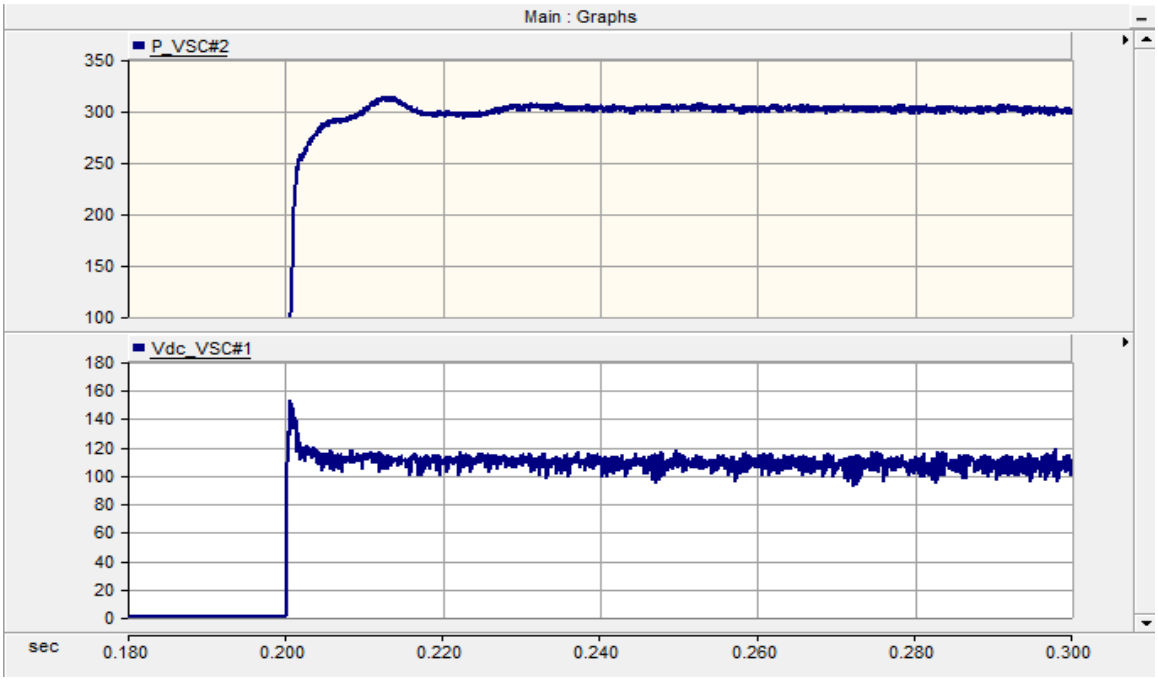

C_{DC} =5 µF

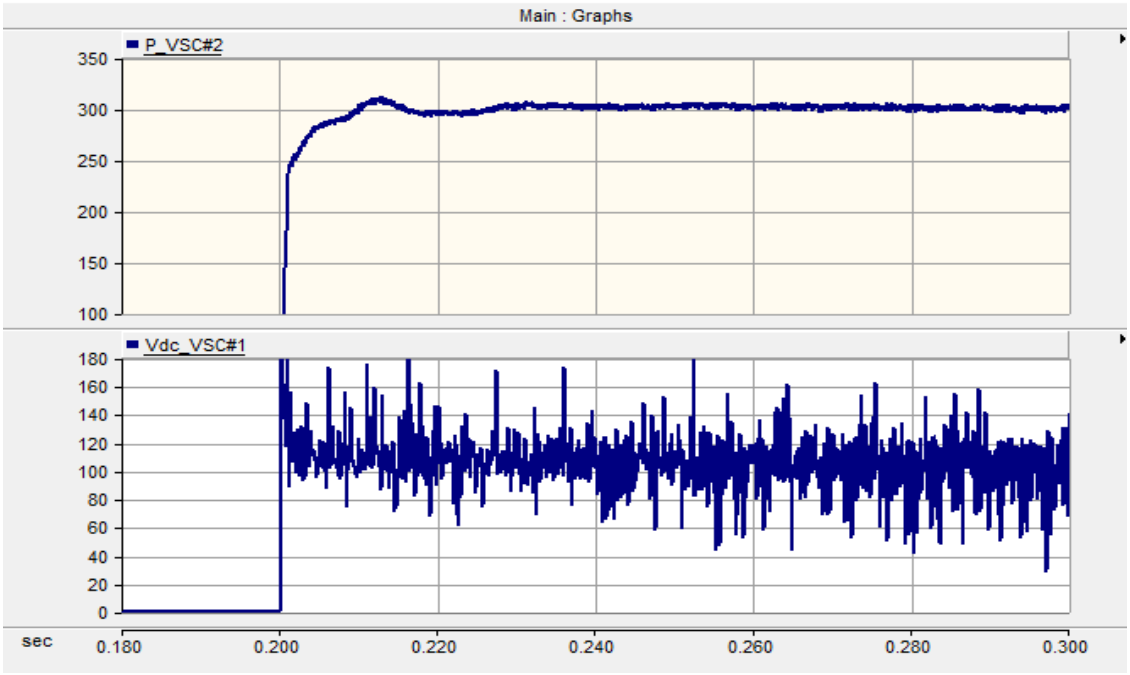

BIBLIOGRAPHY

[1] Chien, Chang Hsin, and R. Bucknall. "Analysis of Harmonics in Subsea Power Transmission Cables Used in VSC–HVDC Transmission Systems Operating Under Steady-State Conditions." *IEEE Transactions on Power Delivery* (IEEE) 22, no. 4 (Oct 2007): 2489 - 2497.

[2] Harnefors, L., N. Johansson, L. Zhang, and B. Berggren. "Interarea Oscillation Damping Using Active-Power Modulation of Multiterminal HVDC Transmissions." *IEEE Transactions* on *Power Systems* (IEEE) PP, no. 99 (Feb 2014): 1-10.

[3] Egea-Alvarez, A., F. Bianchi, A. Junyent-Ferre, G. Gross, and O. Gomis-Bellmunt. "Voltage Control of Multiterminal VSC-HVDC Transmission Systems for Offshore Wind Power Plants: Design and Implementation in a Scaled Platform." *IEEE Transactions on Industrial Electronics* (IEEE) 60, no. 6 (2013): 2381 - 2391.

[4] de la Villa Jaen, A., E. Acha, and A.G. Exposito. "Voltage Source Converter Modeling for Power System State Estimation: STATCOM and VSC-HVDC." *IEEE Transactions on Power Systems* (IEEE) 23, no. 4 (Nov 2008): 1552 - 1559.

[5] Liu, Chongru, Anjan Bose, and Pengfei Tian. "Modeling and Analysis of HVDC Converter by Three-Phase Dynamic Phasor." *IEEE Transactions on Power Delivery* (IEEE) 29, no. 1 (Feb 2014): 3-12.

[6] Pizano-Martinez, A., C.R. Fuerte-Esquivel, H. Ambriz-Perez, and E. Acha. "Modeling of VSC-Based HVDC Systems for a Newton-Raphson OPF Algorithm." *IEEE Transactions on Power Systems* (IEEE) 22, no. 4 (Nov 2007): 1794 - 1803.

[7] Lu, Weixing, and Boon-Teck Ooi. "DC overvoltage control during loss of converter in multiterminal voltage-source converter-based HVDC (M-VSC-HVDC)." *IEEE Transactions on Power Delivery* (IEEE) 18, no. 3 (Jul 2003): 915 - 920.

[8] de Andrade, L., and T.P. de Leao. 2012. "A brief history of direct current in electrical power systems." *IEEE* 1-6.

[9] Hingorani, Narain G., and Laszlo Gyugyi. 2000. *Understanding FACTS.* New York: Institute of Electronics Engineers, Inc.

[10] Flourentzou, N., V.G. Agelidis, and G.D. Demetriades. 2009. "VSC-Based HVDC Power Transmission Systems: An Overview." *IEEE* 592-602.

[11] Zhang, Xiao-Ping. 2004. "Multiterminal Voltage-Sourced Converter-Based HVDC Models for Power Flow Analysis." *IEEE* 1877-1884.

[12] Chaudhuri, Nilanjan Ray, Balarko Chaudhuri, Rajat Majumder, and Amirnaser Yazdani. 2014. *Multi-terminal Direct-Current Grids.* New Jersey: John Wiley & Sons,Inc.

VITA

Mohammed Mabrook Alharbi was born on March 8, 1988 in Riyadh, Saudi Arabia. His high school education was completed in Prince Mohammed bin Saud Al-Kabeer, Riyadh, Saudi Arabia. He received his Bachelor of Engineering degree in Electrical Engineering from the King Saud University, Riyadh, Saudi Arabia in June 2010. In August 2012, he began his Master of Science program in Electrical Engineering at Missouri University of Science and Technology. He obtained his Master's degree in December 2014.